

The Hamburg/ESO R-process Enhanced Star survey (HERES)^{*}

I. Project description, and discovery of two stars with strong enhancements of neutron-capture elements

N. Christlieb^{1,3}, T. C. Beers², P. S. Barklem³, M. Bessell⁴, V. Hill⁵, J. Holmberg^{6,7}, A. J. Korn^{3,8},
B. Marsteller², L. Mashonkina^{9,8}, Y.-Z. Qian¹⁰, S. Rossi¹¹, G. J. Wasserburg¹², F.-J. Zickgraf¹,
K.-L. Kratz^{13,14}, B. Nordström^{6,15}, B. Pfeiffer^{13,14}, J. Rhee^{16,17}, and S. G. Ryan¹⁸

¹ Hamburger Sternwarte, Universität Hamburg, Gojenbergsweg 112, 21029 Hamburg, Germany
e-mail: nchristlieb@hs.uni-hamburg.de

² Department of Physics and Astronomy, Michigan State University, East Lansing, MI 48824, USA

³ Department of Astronomy and Space Physics, Uppsala University, Box 515, 75120 Uppsala, Sweden

⁴ Research School of Astronomy & Astrophysics, Australian National University, Cotter Road, Weston, ACT 2611, Australia

⁵ Observatoire de Paris, GEPI and URA 8111 du CNRS, 92195 Meudon Cedex, France

⁶ Astronomical Observatory, NBIfAFG, Juliane Meries Vej 30, 2100 Copenhagen, Denmark

⁷ Nordic Optical Telescope Scientific Association, Apartado 474, 38 700 Santa Cruz de La Palma, Spain

⁸ Universitäts-Sternwarte München, Scheinerstrasse 1, 81679 München, Germany

⁹ Institute of Astronomy, Russian Academy of Sciences, Pyatnitskaya 48, 109017 Moscow, Russia

¹⁰ School of Physics and Astronomy, University of Minnesota, Minneapolis, MN 55455, USA

¹¹ Departamento de Astronomia Instituto de Astronomia, Geofísica e Ciências Atmosféricas, Universidade de São Paulo, 05508-900 São Paulo SP, Brazil

¹² Division of Geophysics and Planetary Sciences, California Institute of Technology, Pasadena, CA91125, USA

¹³ Institut für Kernchemie, Universität Mainz, 55128 Mainz, Germany

¹⁴ VISTARS HGF – Virtual Institute for Nuclear Structure and Nuclear Astrophysics, Mainz, Germany

¹⁵ Lund University Box 43, 22100 Lund, Sweden

¹⁶ Center for Space Astrophysics, Yonsei University, Seoul 120-749, Korea

¹⁷ Space Astrophysics Laboratory, California Institute of Technology, MC 405-47, Pasadena, CA 91125, USA

¹⁸ Department of Physics and Astronomy, Open University, Walton Hall, Milton Keynes, MK7 6AA, UK

Received 25 June 2004 / Accepted 11 August 2004

Abstract. We report on a dedicated effort to identify and study metal-poor stars strongly enhanced in r -process elements ($[r/Fe] > 1$ dex; hereafter r -II stars), the Hamburg/ESO R-process Enhanced Star survey (HERES). Moderate-resolution ($\sim 2 \text{ \AA}$) follow-up spectroscopy has been obtained for metal-poor giant candidates selected from the Hamburg/ESO objective-prism survey (HES) as well as the HK survey to identify sharp-lined stars with $[Fe/H] < -2.5$ dex. For several hundred confirmed metal-poor giants brighter than $B \sim 16.5$ mag (most of them from the HES), “snapshot” spectra ($R \sim 20000$; $S/N \sim 30$ per pixel) are being obtained with VLT/UVES, with the main aim of finding the 2–3% r -II stars expected to be among them. These are studied in detail by means of higher resolution and higher S/N spectra. In this paper we describe a pilot study based on a set of 35 stars, including 23 from the HK survey, eight from the HES, and four comparison stars. We discovered two new r -II stars, CS 29497–004 ($[Eu/Fe] = 1.64 \pm 0.22$) and CS 29491–069 ($[Eu/Fe] = 1.08 \pm 0.23$). A first abundance analysis of CS 29497–004 yields that its abundances of Ba to Dy are on average enhanced by 1.5 dex with respect to iron and the Sun and match a scaled solar r -process pattern well, while Th is underabundant relative to that pattern by 0.3 dex, which we attribute to radioactive decay. That is, CS 29497–004 seems not to belong to the class of r -process enhanced stars displaying an “actinide boost”, like CS 31082–001 (Hill et al. 2002), or CS 30306–132 (Honda et al. 2004b). The abundance pattern agrees well with predictions of the phenomenological model of Qian & Wasserburg.

Key words. surveys – stars: abundances – stars: population II – Galaxy: abundances – Galaxy: halo

1. Introduction

^{*} Based in large part on observations collected at the European Southern Observatory, Paranal, Chile (proposal number 68.B-0320).

In the past few years a great deal of attention has become focused on the very rare class of objects known as the

“*r*-process-enhanced metal-poor” stars. These objects are enormously important as they allow to study, among other things, the nature of the rapid neutron-capture process(es), and possibly identify the site(s) for this nucleosynthesis process(es). Furthermore, and perhaps even more importantly, individual age determinations are possible for these stars using long-lived radioactive isotopes, such as ^{232}Th (half-life 14.05 Gyr) or ^{238}U (4.468 Gyr). By comparing the abundance ratio of these elements relative to a stable *r*-process element of similar mass to the production ratio expected from theoretical *r*-process yields, the time elapsed since the nucleosynthesis event that produced these elements took place (e.g., in a type-II supernova) can be derived. The time between this nucleosynthesis event and the birth of stars that formed from gas clouds enriched by this material, including the low-mass, *r*-process-enhanced stars that we observe today, is considered as negligible compared to the age of the star. Therefore, abundance ratios like Th/Eu, U/Eu, or U/Th can be used as chronometers for age determination of *r*-process-enhanced stars.

For ease of discussion, we divide the *r*-process enhancement phenomenon in metal-poor stars into two categories:

r-I: metal-poor stars with $+0.3 \leq [\text{Eu}/\text{Fe}] \leq +1.0$ and $[\text{Ba}/\text{Eu}] < 0$;

r-II: metal-poor stars with $[\text{Eu}/\text{Fe}] > +1.0$ and $[\text{Ba}/\text{Eu}] < 0$.

Note that the term “metal-poor” is not necessarily referring to the overall metal-content of the star, which might in fact not be significantly below the solar value when the star under consideration also has strong overabundances of C, N, and O. We use Eu as reference element for the neutron-capture elements which were mainly produced by the *r*-process in the solar material, because its abundance is most easily measurable. We include the condition $[\text{Ba}/\text{Eu}] < 0$ into the above definitions, because Eu *can* be produced by the *s*-process as well. Therefore we need to distinguish between “pure” *r*-process-enhanced stars and stars that were enriched by material produced in the *r*- and *s*-process (like CS 22948–27 and CS 29497–34, and HE 2148–1247; see Hill et al. 2000; and Cohen et al. 2003, respectively), or only by the *s*-process. Adopting the values of Burris et al. (2000) for the solar Ba and Eu abundances and *r*- and *s*-fractions of these elements, it follows that a star purely enriched by neutron-capture elements produced in the *s*-process would have $[\text{Ba}/\text{Eu}]_s = +1.5$, while $[\text{Ba}/\text{Eu}]_r = -0.82$ for a pure *r*-process star.

It is not yet clear whether the division between r-I and r-II stars is physically meaningful, in the sense that the r-I and r-II stars are associated with different nucleosynthetic histories. It is not even clear whether the distribution of *r*-process-element enhancements, relative to iron, is best described as bimodal. For now, this is only a division of convenience.

The first r-II star, CS 22892–052, was originally identified in the compilation of metal-poor HK survey objects of Beers et al. (1992). At that time it stood out because of its unusually strong CH *G*-band for its low metallicity ($[\text{Fe}/\text{H}] = -3.1$). Soon afterwards, it was observed at high resolution by McWilliam et al. (1995). It was immediately apparent that CS 22892–052 was clearly of interest for other reasons as well – the strength of absorption features associated with the *r*-process, such as Eu II,

were far greater than had been previously observed in giants of such low metallicity.

Sneden et al. (1996) showed that numerous other elements, including some never detected before in metal-poor stars (such as Tb, Ho, Tm, Hf, and Os) exhibited abundances, relative to iron, that were between 30 and 50 times greater than observed in the Sun ($+1.2 \leq [r\text{-process}/\text{Fe}] \leq +1.6$), making it a completely unique object at the time. Of further interest, an absorption line of Th was of measurable strength, which led to the use, by a number of authors, of the Th/Eu chronometer to estimate the age of this star (Sneden et al. 1996; Cowan et al. 1997, 1999; Sneden et al. 2003). This permitted, for the first time in an extremely low metallicity star, the use of this technique to place a strong lower limit on the age of the Galaxy, and hence of the Universe. Sneden et al. (2003), using new calculations for the Th/Eu production ratio, determined an age of 12.8 ± 3 Gyr for CS 22892–052. In the cosmological model fit to data recently obtained with the Wilkinson Microwave Anisotropy Probe, and extensive redshift-survey data, the age of the Universe is 13.7 ± 0.2 Gyr, which is consistent with the lower limit following from the age of CS 22892–052.

Fortunately, CS 22892–052 is not unique. During the course of a Large Programme of Cayrel et al. (“First Stars”) carried out at the European Southern Observatory (ESO), high-resolution observations of the very metal-poor ($[\text{Fe}/\text{H}] = -2.9$) giant CS 31082–001 revealed it to be an r-II star as well ($[\text{Eu}/\text{Fe}] = +1.6$). However, in contrast to CS 22892–052, CS 31082–001 is not strongly carbon-enhanced, immediately calling into question any causal connection between the enhancement of carbon and the *r*-process enhancement phenomenon.

In CS 31082–001, it was possible for the first time in a metal-deficient star to detect not only thorium, but also uranium, a potentially much more useful chronometer than Th (Cayrel et al. 2001). The simultaneous detection of U and Th allowed for the first use of the U/Th chronometer, which has less reliance on the uncertain nuclear physics associated with the *r*-process than does the Th/Eu chronometer (e.g., Schatz et al. 2002; Wanajo et al. 2002). However, while $[\text{Eu}/\text{Fe}]$ (and the ratios of other *r*-process elements relative to iron) were enhanced by a similar factor as observed in CS 22892–052, Hill et al. (2002) noted that Th/Fe was almost a factor of three higher than observed in CS 22892–052, i.e., $\log(\text{Th}/\text{Eu}) = -0.22$ as compared to $\log(\text{Th}/\text{Eu}) = -0.62$ in CS 22892–052 (Sneden et al. 2003). This fact makes questionable the use of chronometers such as Th/Eu as well as other alternative chronometer pairs involving the actinides Th or U in combination with lighter elements ($Z \leq 70$). Recent theoretical *r*-process calculations yield a production ratio of $\log(\text{Th}/\text{Eu})_0 = -0.35$ (Sneden et al. 2003), and hence it would follow that CS 31081–001 has a *negative* age.

Honda et al. (2004a,b) recently reported on Subaru/HDS observations of 22 metal-poor stars with $[\text{Fe}/\text{H}] < -2.5$, including eight stars from the HK survey which were not studied at high spectral resolution before. They discovered one new r-I star (CS 30306–132; $[\text{Eu}/\text{Fe}] = +0.85$), and one r-II star (CS 22183–031; $[\text{Eu}/\text{Fe}] = +1.2$). CS 30306–132 is the second star known to be suffering from an “actinide boost”: its

Th/Eu ratio of $\log(\text{Th}/\text{Eu}) = -0.10$ is even higher than the ratio observed in CS 31081–001. Unfortunately the Subaru/HDS spectrum of the r-II star CS 22183–031 available to Honda et al. was not of sufficient quality to detect Th.

Since the discovery of CS 22892–052, and the realization of the potential power of the Th/Eu chronometer, a handful of r-I stars have been discussed in the literature as well (e.g., HD 115444, Westin et al. 2000; BD+17° 3248, Cowan et al. 2002). These stars appear on the whole to be more common than their extreme counterparts. They also provide valuable information, not only through application of the Th/Eu chronometer to obtain age limits, but on the remarkable consistency of the pattern of *r*-process elements from star to star, which follows a scaled solar *r*-process pattern within measurement uncertainties.

In conclusion, larger samples of *r*-process-enhanced metal-poor stars are needed in order to make progress in our understanding of the phenomenon of *r*-process enhancement, investigate how common the “actinide boost” phenomenon is and what its physical reasons might be, identification of reliable chronometers for age determinations, and for constraining what the possible site(s) of the *r*-process(es) are. However, there are several fundamental problems which make the identification and study of these stars a challenge. First of all, they are extremely rare. Based on high-resolution spectroscopy that has been performed on the most metal-deficient giants, it appears that r-II stars occur no more frequently than about one in 30 giants with $[\text{Fe}/\text{H}] < -2.5$, i.e., roughly 3%. Due to the steep decrease of the metallicity distribution of the galactic halo towards low metallicity (Ryan & Norris 1991; Beers 1999), giants in that $[\text{Fe}/\text{H}]$ range are rare themselves, although modern spectroscopic wide-angle surveys, like the HK and Hamburg/ESO (HE) surveys, have succeeded in identifying such stars with success rates as high as 10–20% (Beers 1999; Christlieb 2003). So, we are faced with the daunting prospect of searching for a rare phenomenon amongst rare objects. The r-I stars appear to be found with a frequency that is at least a factor of two greater than this, and fortunately extend into the higher metallicity stars (e.g., BD+17° 3248 with $[\text{Fe}/\text{H}] = -2.1$), where a greater number of candidates exist.

Detection of uranium presents an even bigger challenge, due to the weakness of the absorption lines involved, and blending with features of other species. It was not possible to measure even the strongest uranium line in the optical, U II 3859.57 Å, in the carbon-enhanced star CS 22892–052, because of blending with a CN line. The U line is also close to a strong Fe line at 3859.9 Å (see Fig. 10 of Hill et al. 2002). The ideal star for detecting uranium would therefore be a cool giant with low carbon abundance, very low overall metallicity, but strong enhancement of the *r*-process elements, and it should be a bright star, because high signal-to-noise ratios (S/N) as well as high spectral resolution ($R = \lambda/\Delta\lambda > 60\,000$) are required to measure the U II 3859.57 Å line accurately. Note that in CS 31082–001, this line has an equivalent width of only $\sim 2\text{ m}\text{\AA}$.

These reasons motivated us to start a systematic search for r-II stars. In this paper we describe the approach we have chosen (Sect. 2). We present a sample of stars observed in a pilot

study (Sect. 3), and details of their observations (Sect. 4). We report on the discovery of two new r-II stars, CS 29497–004 ($[\text{Eu}/\text{Fe}] = 1.64 \pm 0.22$) and CS 29491–069 ($[\text{Eu}/\text{Fe}] = 1.08 \pm 0.23$). A first abundance analysis of CS 29497–004, the more strongly *r*-process enhanced star of the two, is described in Sect. 5, and in Sect. 6 we discuss its abundance pattern. We finish our paper with conclusions and remarks on future prospects.

2. The HERES approach

For finding r-II stars, we adopt a two-step approach. The first step consists of the identification of a large sample of metal-poor giants with $[\text{Fe}/\text{H}] < -2.5$ in the Hamburg/ESO Survey (HES), by means of moderate-resolution ($\sim 2\text{ \AA}$) follow-up spectroscopy of several thousand cool ($0.5 < B - V < 1.2$) metal-poor candidates selected in that survey. In the second step, “snapshot” spectra ($S/N \sim 30$ per pixel at 4100 Å; $R \sim 20\,000$) of confirmed metal-poor stars are obtained. Such spectra can be secured for an $B = 15.0$ star with a 8-m-class telescope in exposure times of only 900 s (see Table 2), and under unfavourable observing conditions in terms of seeing, fractional illumination of and distance to the moon, cloud coverage, and airmass. The weak constraints on the observing conditions makes it feasible to observe large samples of stars.

As is demonstrated in Fig. 1, snapshot spectra allow to easily identify stars with enhancements of *r*-process elements, using the Eu II 4129.73 Å line, since this line is very strong in these stars. For example, in CS 22892–52, it has an equivalent width of more than 100 mÅ.

We adopt the snapshot spectroscopy approach in a Large Programme (170.D-0010, P. I. Christlieb) approved by ESO. A total of 373 stars (including 4 comparison stars) are scheduled to be observed; most of them are from the HES. These observations are expected to yield 5–10 new r-II stars, and at least twice as many r-I stars.

As a by-product, our program will provide the opportunity to measure abundances of α -elements such as Mg, Ca, and Ti, iron-peak elements such as Cr, Mn, Fe, Co, Ni, and Zn, as well as other elements, depending on the S/N of each spectrum, for the entire set of stars that we plan to observe in snapshot mode. This will result in by far the largest sample of very metal-poor stars with homogeneously-measured abundances of a significant number of individual elements. Given the large number of spectra to be processed, it is mandatory that we employ automated techniques for abundance analysis. Such techniques are described in a companion paper (Barklem et al. 2004, hereafter Paper II).

3. The pilot study sample

At the end of 2001, i.e., before the ESO Large Programme was approved, a snapshot spectroscopy pilot study was conducted with the Ultraviolet-Visual Échelle Spectrograph (UVES, Dekker et al. 2000) mounted on the 8 m Unit Telescope 2 (Kueyen) of the Very Large Telescope (VLT), in order to verify the feasibility of our approach to find r-II stars. The targets were drawn from lists of confirmed metal-poor stars with $[\text{Fe}/\text{H}] < -2.5$ from the HK and Hamburg/ESO surveys,

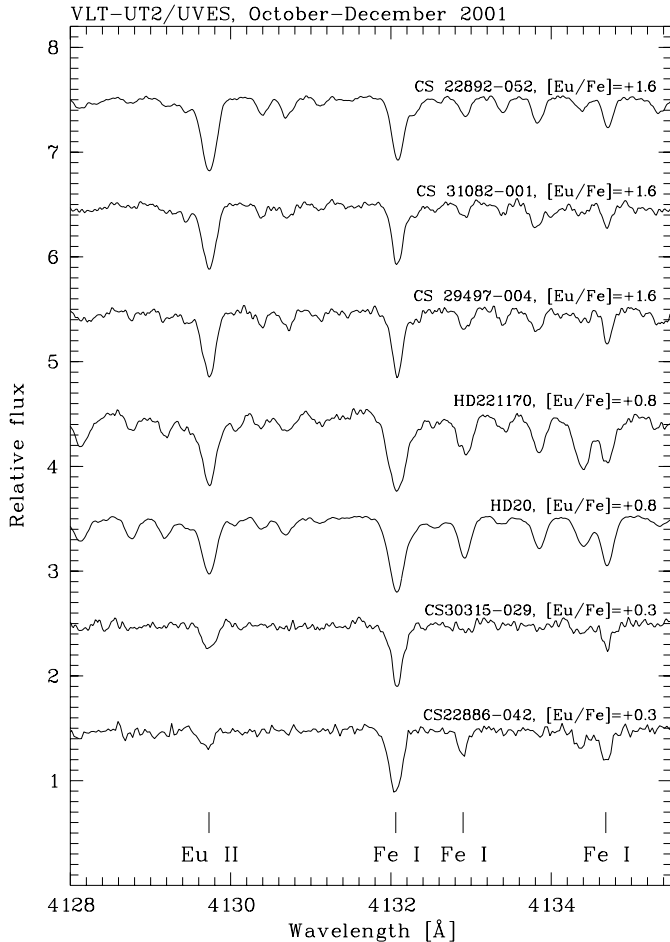


Fig. 1. Spectral region around the Eu II 4129.73 Å line in several known r-I and r-II stars observed in our program for comparison reasons, and stars newly-identified in our pilot study.

where $[Fe/H]$ is determined from moderate-resolution (~ 2 Å) follow-up spectroscopy using the Ca II K technique of Beers et al. (1999). We restricted the sample to stars with $B - V > 0.5$, because we are primarily interested in cool, sharp-lined giants. The $B - V$ colours are based on CCD photometry in case of the HK-survey stars (recognisable by designations beginning with “CS” for Curtis Schmidt-telescope), or were derived directly from the HES objective-prism spectra, in case of the HES stars (designations beginning with “HE”)¹. Despite of this colour selection, two stars later turned out to be dwarfs and a few to be subgiants hotter than desired (for details see Table 4 of Paper II). The main reason for this is that the HES $B - V$ colours are of limited accuracy, i.e., $\sigma = 0.1$ mag (Christlieb et al. 2001).

35 stars successfully observed with VLT/UVES for which CCD BVR photometry is available to us form the sample of

¹ The nomenclature adopted in this and the original works on CS stars has been modified when the stars were subsequently incorporated into the SIMBAD database. For reasons associated with the uniqueness of SIMBAD entries, stars which in the literature have designations CS XXXXX-XXX are listed in SIMBAD as BPS CS XXXXX-XXXX.

our pilot study². The sample is presented in Table 1. It includes four comparison stars which are known to be r-I or r-II stars: HD 20 and HD 221170 (Burriss et al. 2000), CS 22892-052 (Snedden et al. 1996, 2000, 2003), and CS 31082-001 (Cayrel et al. 2001; Hill et al. 2002). Three stars, CS 22186-025, CS 30315-029, and CS 30337-097, are included in the ESO Large Programme “The First Stars” of Cayrel et al. Abundances from C to Zn for CS 22186-025 have been published in Cayrel et al. (2004, see that paper for further references for the “First Stars” project).

Based on the results presented in Paper II as well as Sect. 5 below, we classify one of the 31 previously unobserved stars in our sample as an r-I star (CS 30315-029), and two as r-II stars (CS 29497-004³ and CS 29491-069).

4. Observations

Moderate-resolution spectroscopic follow-up observations were carried out in numerous campaigns with a variety of telescope/instrument combinations, including the SSO 2.3 m/DBS, ESO 3.6 m/EFOSC2, ESO NTT/EMMI, ESO 1.5 m/B&C Spectrograph, McDonald 2.7 m/LCS, the R-C spectrographs mounted at the KPNO 4 m, KPNO 2.1 m, CTIO 4 m and CTIO 1.5 m telescopes.

The VLT/UVES observations of the pilot study sample were carried out between 7 October and 4 December 2001. We used the BLUE 437 setup, yielding a wavelength coverage of $\lambda = 3760\text{--}4980$ Å. A 2'' slit was chosen, typically yielding (seeing-limited) resolving powers of $R = 20\,000\text{--}25\,000$. While acquiring the data, the CCD binning was set to 1×1 pixels, which results in oversampling in combination with the wide slit. Therefore, we rebinned the pipeline-reduced spectra by a factor of two. The exposure times were set such that a minimum nominal S/N per rebinned pixel of 20 was reached, assuming a seeing of 2'', full moon, thin cirrus, and $\sec z = 2$. However, given that the overhead for telescope pointing, image analysis, target acquisition, CCD readout, etc., is ~ 10 min, the minimum exposure time was set to 10 min (except for the very bright stars HD 20 and HD 221170, which would saturate the detector in this exposure time) to avoid inefficient use of the telescope time. This resulted in $S/N > 50$ for some of the brighter stars. Furthermore, if the observing conditions were better than assumed in our exposure time calculations, higher S/N spectra were acquired. The observations are summarized in Table 2.

CCD BVR photometry was obtained at the ESO-Danish 1.54 m-telescope with DFOSC. The observers were Beers & Rossi (runs in December 1998, 2000), Holmberg (October 2002 and April 2003 runs) and Zickgraf (October 2003 run). The data was reduced using the usual

² For completeness we mention that one additional star has been removed from the sample because we found it to have a surface gravity of $\log g = 4.9$, which is not covered by our grid of model atmospheres described in Paper II, and it appeared to be a fast rotator, making an automated abundance analysis difficult.

³ CCD photometry for this star has been previously reported by Norris et al. (1999).

Table 1. The pilot study sample. Coordinates of the HES stars have been derived from the Digitized Sky Survey I and are accurate to $1''$. The coordinates of the HK survey stars are from identifications of the sources in the 2MASS All Sky Release. V magnitudes and $B - V$ colours have been measured with CCD photometry; $[\text{Fe}/\text{H}]$ is derived from moderate-resolution follow-up spectroscopy using the methods of Beers et al. (1999). The photometry for HD 20 and HD 221170 has been retrieved from SIMBAD. Note that $[\text{Fe}/\text{H}]$ as listed here was determined by using the most recent follow-up spectra as well as updates of the programs of Beers et al. (1999), therefore the metallicities have changed by a few tenths of a dex in some cases. The best available $[\text{Fe}/\text{H}]$ for the stars with $[\text{Fe}/\text{H}] > -2.5$ in the table was below -2.5 dex when the target selection was done.

Star	α (2000.0)	δ (2000.0)	V	$B - V$	$[\text{Fe}/\text{H}]$	Note
CS 22175-007	02 17 26.6	-09 00 45	13.461	0.676	-2.63	
CS 22186-023	04 19 45.5	-36 51 35	12.841	0.682	-2.72	
CS 22186-025	04 24 32.8	-37 09 02	14.228	0.737	-2.77	Cayrel et al. LP
CS 22886-042	22 20 25.8	-10 23 20	13.263	0.831	-2.53	
CS 22892-052	22 17 01.6	-16 39 27	13.213	0.800	-2.97	r-II (comparison star)
CS 22945-028	23 31 13.5	-66 29 57	14.624	0.653	-2.38	
CS 22957-013	23 55 49.0	-05 22 52	14.089	0.775	-2.86	
CS 22958-083	02 15 42.7	-53 59 56	14.423	0.664	-2.68	
CS 22960-010	22 08 25.3	-44 53 56	13.944	0.497	-2.15	
CS 29491-069	22 31 02.1	-32 38 36	13.075	0.600	-2.81	r-II
CS 29491-109	22 25 01.1	-32 14 41	13.181	0.802	-2.37	
CS 29497-004	00 28 06.9	-26 03 04	14.034	0.705	-2.66	r-II
CS 29510-058	02 21 46.5	-24 01 58	13.510	0.669	-2.62	
CS 30308-035	20 45 54.1	-44 50 29	13.850	0.788	-3.23	
CS 30315-001	23 37 38.8	-26 21 53	13.763	0.902	-2.73	
CS 30315-029	23 34 26.6	-26 42 14	13.661	0.915	-3.29	r-I; Cayrel et al. LP
CS 30337-097	22 01 21.5	-30 57 57	13.202	0.722	-2.65	Cayrel et al. LP
CS 30339-041	00 23 12.9	-37 01 26	13.915	0.555	-2.42	
CS 30343-063	21 45 17.5	-37 22 18	13.008	1.045	-2.58	
CS 31060-047	00 08 07.8	-15 54 03	13.823	0.854	-2.87	
CS 31062-041	00 35 03.0	-15 54 29	13.934	0.820	-3.02	
CS 31072-118	05 08 53.5	-59 18 21	12.695	0.920	-2.94	
CS 31082-001	01 29 31.1	-16 00 45	11.666	0.766	-2.80	r-II (comparison star)
HD 20	00 05 15.3	-27 16 18	9.07	0.54	-1.25	r-I (comparison star)
HD 221170	23 29 28.8	+30 25 57	7.71	1.02	-1.61	r-I (comparison star)
HE 0109-3711	01 11 38.4	-36 55 17	16.290	0.378	-3.00	
HE 0131-2740	01 33 25.8	-27 25 28	14.632	0.590	-2.70	
HE 0249-0126	02 51 39.7	-01 14 33	15.685	0.571	-2.52	
HE 0256-1109	02 59 10.1	-10 58 01	15.608	0.549	-2.75	
HE 0447-4858	04 49 01.0	-48 53 35	16.254	0.433	-2.03	
HE 0501-5139	05 02 48.1	-51 35 36	16.094	0.479	-2.86	
HE 0513-4557	05 15 12.1	-45 54 10	15.743	0.536	-3.00	
HE 0519-5525	05 19 59.1	-55 22 41	15.034	0.536	-2.42	
HE 2145-3025	21 48 43.3	-30 11 08	14.879	0.533	-2.40	
HE 2338-1311	23 41 08.3	-12 55 10	15.622	0.597	-2.85	

IRAF photometry reduction packages. The stars were calibrated to the $BVR_C I_C$ system, (where the subscript “C” indicates Kron-Cousins) using a selection of stars from nightly observations of Landolt standard fields. Typical errors in the resulting magnitudes are of the order of 0.01–0.02 mag, i.e.,

better than the uncertainties expected to arise from reddening corrections. For further details, see Beers et al. (2004, in preparation). V magnitudes and $B - V$ colours are listed in Table 1; additional colours can be found in Table 3 of Paper II.

Table 2. Observations of the pilot study sample. UT is the Universal Time at the start of the observations; S/N is the average signal-to-noise ratio per rebinned pixel in order #113 ($\lambda = 4112.3\text{--}4148.9 \text{ \AA}$).

Star	Date	UT	t_{exp} [s]	S/N
CS 22175–007	2001–11–23	00:50:07	600	28
CS 22186–023	2001–10–10	08:50:08	600	51
CS 22186–025	2001–10–08	08:52:52	900	29
CS 22886–042	2001–11–29	00:50:15	600	36
CS 22892–052	2001–11–01	00:33:42	600	41
CS 22945–028	2001–12–02	02:04:55	900	27
CS 22957–013	2001–11–22	02:03:40	900	31
CS 22958–083	2001–11–01	03:44:10	900	29
CS 22960–010	2001–10–07	03:08:57	900	32
CS 29491–069	2001–12–02	01:49:30	600	51
CS 29491–109	2001–12–02	01:32:46	600	44
CS 29497–004	2001–11–01	03:04:07	900	35
CS 29510–058	2001–11–23	05:43:00	600	34
CS 30308–035	2001–11–01	00:02:09	600	29
CS 30315–001	2001–12–02	02:25:14	600	32
CS 30315–029	2001–12–03	00:45:57	600	33
CS 30337–097	2001–10–07	02:53:24	600	40
CS 30339–041	2001–11–01	02:45:56	600	34
CS 30343–063	2001–10–07	02:37:17	600	34
CS 31060–047	2001–11–22	00:42:29	600	26
CS 31062–041	2001–11–01	03:24:03	900	33
CS 31072–118	2001–10–09	08:47:15	600	47
CS 31082–001	2001–11–22	01:01:11	600	81
HD 20	2001–12–04	00:32:44	60	101
HD 221170	2001–11–22	00:33:55	10	40
HE 0109–3711	2001–11–23	03:05:57	1800	16
HE 0131–2740	2001–11–23	02:37:45	1200	26
HE 0249–0126	2001–11–23	01:34:02	1200	12
HE 0256–1109	2001–11–23	02:00:28	1200	15
HE 0447–4858	2001–11–23	03:42:26	1800	16
HE 0501–5139	2001–11–13	07:53:40	1800	20
HE 0513–4557	2001–11–12	05:18:27	1200	18
HE 0519–5525	2001–11–17	07:53:23	1200	24
HE 2145–3025	2001–11–01	00:48:50	900	24
HE 2338–1311	2001–11–01	01:08:34	1200	19

5. Abundance analysis of CS 29497–004, a new r-II star

A quick-look analysis of the snapshot spectrum of CS 29497–004, based on the equivalent ratio of the Eu II 4129 and Fe I 4132 lines immediately revealed that this star is strongly enhanced in neutron-capture elements. We therefore carried out a first abundance analysis. A more comprehensive

Table 3. Stellar parameters adopted for CS 29497–004.

Colour	Value	T_{eff}
$(V - J)_0$	1.539 ± 0.029	$5035 \pm 75 \text{ K}$
$(V - K)_0$	2.066 ± 0.032	$5110 \pm 50 \text{ K}$

analysis, based on higher resolution and S/N data already obtained with VLT/UVES, will be presented in a forthcoming paper (Hill et al. 2004, in preparation).

For the abundance analysis we used spherically symmetric model atmospheres from a new grid of MARCS models (Gustafsson et al. 2004). Enhancement of α -elements by +0.4 dex has been taken into account.

5.1. Stellar parameters

The effective temperature T_{eff} was derived from broad-band visual (V) and infrared (JK) photometry with the methods described in Cohen et al. (2002). The JK measurements are from the Two Micron All Sky Survey⁴ (2MASS; Skrutskie et al. 1997). From the maps of Schlegel et al. (1998) we computed $E(B - V) = 0.016$ for the interstellar reddening along the line of sight to CS 29497–004, and we de-reddened the $V - J$ and $V - K$ colours using this value. The results are listed in Table 3.

We adopt the weighted average of the effective temperatures deduced from these colours, $T_{\text{eff}} = 5090 \text{ K}$. The formal error for T_{eff} is small, i.e., of the order of 50 K, but a comparison with values deduced from Balmer line profile analysis as well as the photometrically determined value of 5013 K reported in Paper II reveals that systematic errors might be larger, of the order of $\sim 100 \text{ K}$.

Surface gravities $\log g$ can be determined from the Fe I/Fe II ionisation equilibrium. Fe I is, however, a minority species in cool giants and therefore potentially subject to formation under non-LTE conditions which could affect gravity estimates in a systematic way. Fe I non-LTE calculations for metal-poor stars were recently carried out by Korn et al. (2003). Applying these calculations (updated with respect to the treatment of Rayleigh scattering) to CS 29497–004, we find non-LTE corrections for the Fe I abundance of +0.10 dex, corresponding to a correction in $\log g$ of +0.25 dex. An analysis differentially to the Sun performed by A. Korn with a plane-parallel MAFAGS model (Gehren 1975a,b) led to a non-LTE gravity of $\log g = 2.25$, where both Fe I and Fe II give $[\text{Fe}/\text{H}] = -2.63 \pm 0.09$. Inspection of a 12 Gyr isochrone for $Z = 0.00001 Z_{\odot}$ (Yi et al. 2001) reveals that a star of $T_{\text{eff}} = 5090 \text{ K}$ on the giant branch has $\log g = 2.28$, in very good agreement with the non-LTE analysis. The non-differential analysis resulted in $\log g = 2.35$. The determination by A. Korn was limited to 14 Fe I and 7 Fe II lines in the yellow spectral region which were chosen based on their relatively undisturbed

⁴ 2MASS is a joint project of the University of Massachusetts and the Infrared Processing and Analysis Center/California Institute of Technology, funded by the National Aeronautics and Space Administration and the US National Science Foundation.

Table 4. Stellar parameters adopted for CS 29497–004.

Parameter	Value	σ
T_{eff}	5090 K	100 K
$\log g$ (cgs)	2.4 dex	0.4 dex
$[\text{Fe}/\text{H}]_{\text{LTE}}$	−2.64 dex	0.12 dex
v_{micr}	1.6 km s ^{−1}	0.2 km s ^{−1}

line profiles in the solar spectrum. Many more Fe I lines are available in the blue part of the spectrum of CS 29497–004 (heavily blended at solar metallicity). Using this extended line list with $\log gf$ values from the sources listed in Tables 7–9 of Paper II and spherically-symmetric MARCS models, the Fe I/Fe II ionisation equilibrium is reached at $\log g = 2.4$. Applying the non-LTE correction of +0.25 dex to this value would result in an unrealistically high gravity of $\log g = 2.65$, as judged by the comparison with isochrones. Therefore, and for self-consistency reasons, we adopt the non-differential LTE gravity of $\log g = 2.4$ derived with the MARCS models we also use in our abundance analysis. The formal uncertainty, derived from the uncertainties of the abundances of Fe I and Fe II (see Table 5), is $\Delta \log g = 0.4$ dex.

The LTE iron abundance we derive from the UVES snapshot spectra is $[\text{Fe}/\text{H}] = -2.64 \pm 0.12$, which agrees very well with the value of $[\text{Fe}/\text{H}] = -2.66 \pm 0.3$ we found from moderate-resolution follow-up spectroscopy (see Table 1).

The stellar parameters adopted for our first abundance analysis of CS 29497–004 are summarized in Table 4.

5.2. Abundances of carbon to dysprosium

From the UVES snapshot spectra of CS 29497–004 we derive abundances for 18 elements, including 11 neutron-capture elements. For most of them, we measured equivalent widths of clean lines by fitting simultaneously a Gaussian profile and a local straight-line continuum. We used the line list presented in Paper II, with the exception of the lines employed in spectrum synthesis calculations for the wavelength region around the Th II 4019 Å line (see Sect. 5.3 below).

Hyperfine-structure (HFS) splitting has been taken into account for Sr, Ba and Eu (for sources of the HFS calculations and $\log gf$ values of the lines we used see Paper II). We assume a pure r -process isotopic mixture for Ba and Eu, and solar isotopic ratios for Sr. The abundances of these elements have been determined by spectrum synthesis of the following lines: Ba II 4554.00 Å, Ba II 4934.10 Å, Eu II 3819.67 Å, Eu II 4129.72 Å, and Sr II 4215.54 Å. We note that the Sr and Ba abundances have a considerable sensitivity against changes in the microturbulence. Varying v_{micr} by 0.2 km s^{−1} results in changes of the Ba and Sr abundance (as determined from the lines at 4215 Å and 4554 Å, respectively) of 0.1 dex. In contrast, the effect on the Eu II 4129.72 Å is very small, i.e., $\Delta \log \epsilon / \Delta v_{\text{micr}} = 0.01 \text{ dex} / 0.2 \text{ km s}^{-1}$.

The carbon abundance of CS 29497–004 was measured from CH features around 4323 Å. In Fig. 2 we show a comparison of that spectral region in CS 29497–004 with that

Table 5. LTE abundances of CS 29497–004. σ refers to the 1- σ line-to-line scatter in case of equivalent-width based analysis. In case of the spectrum synthesis results, errors were roughly estimated from the sensitivity of the line strengths to changes of the abundances. In the computation of $[\text{X}/\text{Fe}]$, we compared the abundances of neutral species with $\log \epsilon$ (Fe I), and the abundances of singly ionized species with $\log \epsilon$ (Fe II).

Species	N_{lines}	$\log \epsilon$	$\sigma_{\log \epsilon}$	$(\log \epsilon)_{\odot}$	$[\text{X}/\text{H}]$	$[\text{X}/\text{Fe}]$
CH	syn	5.86	0.10	8.39	−2.53	+0.10
Mg I	4	5.21	0.14	7.58	−2.37	+0.26
Ca I	5	4.04	0.17	6.36	−2.32	+0.31
Ti I	3	2.46	0.07	4.99	−2.53	+0.10
Ti II	8	2.67	0.15	4.99	−2.32	+0.32
VI	1	1.37		4.00	−2.63	0.00
Fe I	28	4.82	0.16	7.45	−2.63	
Fe II	7	4.81	0.12	7.45	−2.64	
Zn I	1	2.20		4.60	−2.40	+0.23
Sr II	syn (1)	0.88	0.20	2.97	−2.09	+0.55
Y II	4	0.30	0.06	2.24	−1.94	+0.70
Zr II	2	0.98		2.60	−1.62	+1.02
Ba II	syn (2)	0.50	0.20	2.13	−1.63	+1.01
Ce II	4	0.07	0.05	1.58	−1.51	+1.13
Nd II	9	0.23	0.12	1.50	−1.27	+1.37
Sm II	2	0.05		1.01	−0.96	+1.68
Eu II	syn (2)	−0.45	0.20	0.51	−0.96	+1.68
Gd II	1	0.27		1.12	−0.85	+1.79
Dy II	1	0.38		1.14	−0.76	+1.88
Th II	syn (1)	−0.96	0.15	0.12	−1.08	+1.56

of CS 22892–052 and CS 31082–001. The CH features in CS 29497–004 are much weaker than in CS 22892–052 and about as weak as in CS 31082–001, making CS 29497–004 a good candidate for an attempt to detect uranium. We derived $\log \epsilon(\text{C}) = 5.86$ for CS 29497–004. For comparison, the C abundances of CS 22892–052 and CS 31082–001 are $\log \epsilon(\text{C}) = 6.30$ (Snedden et al. 2003) and $\log \epsilon(\text{C}) = 5.82$ (Hill et al. 2002), respectively.

From the absence of ¹³CH features in the spectral region around 4224 Å as well as the best fit we could achieve in the wavelength region around the Th II 4019 Å line (see below), we derive a lower limit for the ¹²C/¹³C ratio of 10.

5.3. Spectrum synthesis of the Th II 4019 Å region

We detected the Th II 4019.129 Å line in the UVES snapshot spectrum of CS 29497–004, and carried out a spectrum synthesis of the spectral region around this line (see Fig. 3). It is blended with lines of other species. In particular, in metal-poor, r -process enhanced stars the Ce II line at 4019.057 Å (Snedden et al. 1996), and a ¹³CH line at 4019.000 Å (Norris et al. 1997) have to be taken into account. We used in our spectrum synthesis calculation the line list and atomic data

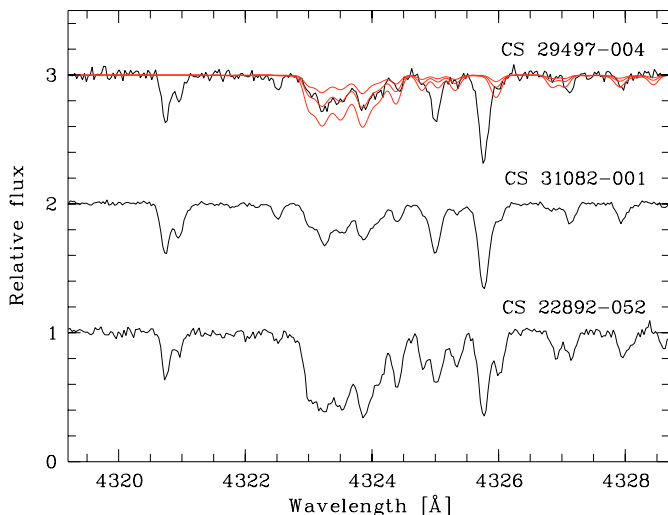


Fig. 2. The CH feature at ~ 4323 Å in CS 29497–004, CS 22892–052 and CS 31082–001. For CS 29497–004, we show a comparison with synthetic spectra computed with $\log \epsilon(\text{C}) = 5.56, 5.86,$ and 6.16 .

of Johnson & Bolte (2001) for this spectral region, supplemented by a few additional, weak lines identified with the Vienna Atomic Line Database⁵ (VALD; Kupka et al. 1999, 2000). Whenever the atomic data retrieved from VALD disagreed with those listed in Johnson & Bolte, we adopted the former. This was the case only for very few lines.

The most important case is the Ce II 4019.057 Å line, for which we adopt the VALD value of $\log gf = -0.213$. This is 0.306 dex lower than that used by Johnson & Bolte, which in turn goes back to Sneden et al. (1996). The latter authors artificially increased the $\log gf$ value of this line by 0.3 dex to improve their fit to the spectrum of CS 22892–052. However, since Norris et al. (1997) have shown that at least part of the missing absorption on the blue side of the Th line is due to ^{13}CH , we do not use the scaled $\log gf$ value for the Ce line, but that listed in VALD.

For the Th II 4019.129 Å line we use $\log gf = -0.228$ (Nilsson et al. 2002), which is 0.042 dex higher than the value adopted by Johnson & Bolte, and 0.423 dex higher than that listed in VALD.

For the partition functions of thorium we interpolate between the values listed in Table 3 of Morell et al. (1992), which are based on calculations provided by Holweger. In the temperature range covered by our stars, the partition functions for Th II are higher by a factor of 3.6–4.4 than those listed in Irwin (1981), translating to abundance differences of the order of 0.5 dex.

For most of the elements which have lines in the relevant spectral region, abundances were available from clean lines in other wavelength regions. We adopted these abundances for the spectrum synthesis. The abundances of elements which we could not determine from lines in other wavelength regions (e.g., Co, Sc) were set to the solar abundance minus 2.64 dex (i.e., the abundances were scaled to the $[\text{Fe}/\text{H}]$ of CS 29497–004).

We first used $^{12}\text{C}/^{13}\text{C} = 10$ in our spectrum synthesis, as constrained from the absence of ^{13}CH features in other wavelength regions. However, it was found that the fit could be considerably improved when it was assumed that *all* carbon in CS 29497–004 is present in the form of ^{12}C , i.e., $^{12}\text{C}/^{13}\text{C} = \infty$. Hence we adopted this value for our final fit.

The result is $\log \epsilon(\text{Th}) = -0.96$ dex. We estimate the uncertainty to be of the order of 0.15 dex, which includes uncertainties introduced by the fit procedure, continuum placement, and the choice of stellar parameters.

5.4. Non-LTE effects

Non-local thermodynamical equilibrium (non-LTE) line formation calculations for CS 29497–004 have been carried out for Ba II, Eu II, and Sr II using the methods described in Mashonkina et al. (1999), Mashonkina & Gehren (2000), and Mashonkina & Gehren (2001), respectively. A modified version of the code NONLTE3, based on the complete linearization method as described by Auer & Heasley (1976), has been used (Kamp et al. 2004).

In cool giants, Ba II, Eu II and Sr II are all majority species. Therefore, departures from LTE level populations of these species are mainly caused by radiative bound-bound transitions. Non-LTE effects strengthen the Ba II and Sr II lines compared with the LTE case resulting in a negative non-LTE abundance correction $\Delta_{\text{NLTE}} = \log \epsilon_{\text{NLTE}} - \log \epsilon_{\text{LTE}}$ and they weaken the Eu II lines, resulting in a Δ_{NLTE} of opposite sign. According to our calculations for the investigated spectral lines $\Delta_{\text{NLTE}} = -0.09$ dex (Ba II 4554 Å), -0.23 dex (Ba II 4934 Å), $+0.03$ dex (Eu II 4129 Å) and -0.12 dex (Sr II 4215 Å).

6. The abundance pattern of CS 29497–004

In Fig. 4 we show a comparison of the abundance pattern of CS 29497–004 with the solar r -process pattern, as listed in Table 5 of Burris et al. (2000), minus 0.83 dex. This is the average difference between the abundances of Ba to Dy observed in CS 29497–004 and the solar r -process pattern. We use the LTE abundances here, because NLTE calculations are not available to us for all elements for which we have measured abundances. The abundances of the elements $56 \leq Z \leq 66$ in CS 29497–004 match the scaled solar r -process pattern well, while Th is underabundant relative to that pattern by 0.3 dex, most likely due to radioactive decay.

Y is also underabundant, by about 0.5 dex relative to the solar r -process pattern derived by Burris et al. (2000). Hill et al. (2002) investigated the difference of the solar r -process patterns as derived by Burris et al. (2000) and Arlandini et al. (1999). For Y, these patterns differ by ~ 0.5 dex. Hill et al. (2002) also noted that a better match with the observed abundance patterns of CS 22892–052 and CS 31082–001 is reached if the solar r -process pattern of Arlandini et al. (1999) are used. We hence conclude that the underabundance of Y relative to the scaled solar r -process pattern we use can probably not be attributed to a different nucleosynthesis history of this element, but is most likely due to uncertainties in the de-composition of the solar abundance pattern into s - and r -process components.

⁵ <http://www.astro.uu.se/~vald/>

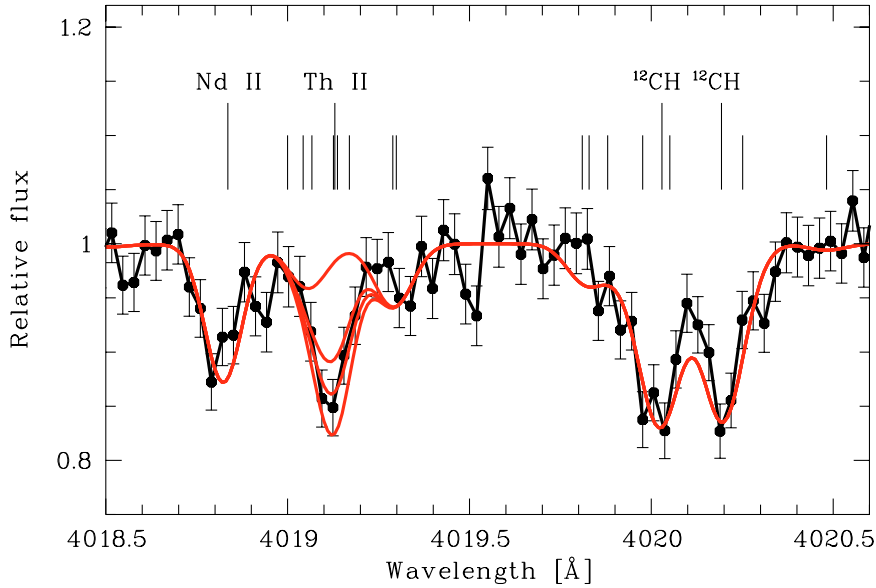


Fig. 3. Spectrum synthesis of the spectral region around Th II 4019 Å in CS 29497–004. The positions of lines that have been taken into account are indicated. The observed spectrum is shown as black line; error bars are the 1σ noise level per pixel. The grey lines are spectrum synthesis results for $\log \epsilon(\text{Th}) = -9.99, -1.11, -0.96$ (best fit), and -0.81 .

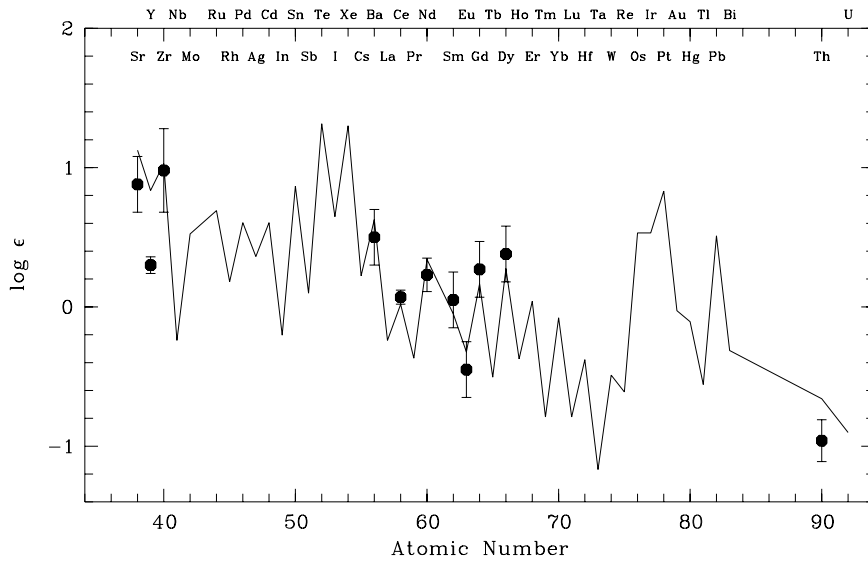


Fig. 4. Abundances of CS 29497–004 compared to the solar r -process abundance pattern, scaled down by 0.83 dex to match the abundances of Ba to Dy in CS 29497–004.

Qian & Wasserburg (2001a,b, 2002) proposed a phenomenological model to explain the abundances of a wide range of elements in metal-poor stars. This model assumes that in general the abundance of an element E in a metal-poor star is given by

$$10^{\log \epsilon(E)} = 10^{\log \epsilon_P(E)} + n_H \times 10^{\log \epsilon_H(E)} + n_L \times 10^{\log \epsilon_L(E)}, \quad (1)$$

where $\log \epsilon_P(E)$ represents the prompt (P) inventory of E in the interstellar medium (ISM) contributed by an early generation of stars, and $\log \epsilon_H(E)$ and $\log \epsilon_L(E)$ represent the yields of E for two hypothesized (H and L) types of core-collapse supernovae that provide the subsequent enrichment of the ISM. The quantities n_H and n_L in Eq. (1) correspond to the “numbers” of H and L events that contributed to the abundances in

the ISM from which the star formed. For CS 29497–004 the model gives $n_H = 107$ and $n_L = 0.3$ if the observed abundances of Eu and Fe are taken to be $\log \epsilon(\text{Eu}) = -0.45$ and $\log \epsilon(\text{Fe}) = 4.81$. Using these values of n_H and n_L and the $\log \epsilon_P$, $\log \epsilon_H$, and $\log \epsilon_L$ values given in Table 3 of Qian & Wasserburg (2001b) and Table 1 of Qian & Wasserburg (2002), the abundances of all the other elements from O to U are calculated from Eq. (1) and presented in Table 6 (an age of 13 Gyr is used to calculate the abundances of Th and U). It can be seen that the model results are in accord with all the data covering the other elements from Mg to Th to within ~ 0.3 dex. We note that the abundances of C and Zn cannot be calculated from Eq. (1) due to incomplete knowledge of the input parameters, especially the relevant $\log \epsilon_L$ values.

Table 6. Abundances of CS 29497–004 compared with predictions of the model of Qian & Wasserburg.

Element	$\log \epsilon$	
	Predicted	Observed
O	6.82	
Na	3.94	
Mg	5.40	5.21 ± 0.14
Al	3.57	
Si	5.33	
Ca	4.10	4.04 ± 0.17
Sc	0.57	
Ti	2.75	2.67 ± 0.15
V	1.65	1.37 ± 0.20
Cr	2.84	
Mn	2.28	
Co	2.32	
Ni	3.44	
Sr	0.87	0.88 ± 0.20
Y	0.06	0.30 ± 0.06
Zr	0.65	0.98 ± 0.20
Nb	-0.53	
Ru	0.48	
Rh	-0.31	
Pd	0.22	
Ag	-0.30	
Cd	0.13	
Ba	0.48	0.50 ± 0.20
La	-0.19	
Ce	0.01	0.07 ± 0.05
Pr	-0.48	
Nd	0.13	0.23 ± 0.12
Sm	-0.17	0.05 ± 0.20
Gd	0.03	0.27 ± 0.20
Tb	-0.67	
Dy	0.11	0.38 ± 0.20
Ho	-0.50	
Er	-0.10	
Tm	-0.90	
Yb	-0.19	
Lu	-0.95	
Hf	-0.58	
Os	0.37	
Ir	0.40	
Pt	0.69	
Au	-0.17	
Th	-0.97	-0.96 ± 0.20
U	-1.74	

In the above model, the values of $n_H = 107$ and $n_L = 0.3$ require that for CS 29497–004, the abundances of the elements from O to Ni be dominated by the P inventory and those of

the elements from Sr to U by contributions from the H events. Further, the extremely high value of $n_H = 107$ can not be attributed to enrichment of the ISM but would indicate that the abundances of the r -process elements in CS 29497–004 are due to the contamination of this star’s surface by a previous H event associated with a binary companion. The question of whether this star is in a binary as evidenced by periodic shift in radial velocity or was in a binary as evidenced by high proper motion should be investigated. Thus, CS 29497–004 belongs to the same class of metal-poor stars with extremely enhanced r -process abundances as CS 22892–052 and CS 31082–001 (see discussion in Qian & Wasserburg 2001a).

We note that the low value of $n_L = 0.3$ calculated for CS 29497–004 based on the model may indicate no L event contributions to this star. Instead, the abundances of the elements from O to Zn in this star may simply reflect a possible range of the P inventory due to variations in the mixing of the contributions from the early generation of stars with the ISM. In this case, the abundances of the elements from O to Zn are given by the relevant $\log \epsilon_P$ values corrected for a dilution factor corresponding to a shift of $\log \epsilon(\text{Fe}) - \log \epsilon_P(\text{Fe}) = 0.3$ dex. The results obtained this way for the elements from O to Ni are essentially the same as those given in Table 6. Further, the abundances of Cu and Zn are calculated to be $\log \epsilon(\text{Cu}) = 0.83$ and $\log \epsilon(\text{Zn}) = 2.16$. The result for Zn is in excellent agreement with the data.

7. Conclusions and outlook

With the discovery of two new r-II stars and one new r-I star, we have demonstrated that it is indeed feasible to identify such stars by means of snapshot spectroscopy. We use this concept in a large-scale observational program – the HERES project – which is currently being carried out with VLT/UVES.

Our pilot project sample contains 23 previously unobserved stars with $[\text{Fe}/\text{H}] < -2.5$, and we found two new r-II stars. This exceeds our previous estimate of the relative frequency of r-II stars of $\sim 3\%$. The full set of 369 HERES stars will allow to determine the relative frequency of r-II and also r-I stars more accurately.

We measured the abundances of 18 elements in CS 29497–004, including 11 neutron-capture elements. The snapshot spectrum we used for our first analysis was obtained with the aim of identifying r-I and r-II stars, and not for age determinations. The limited quality of the spectrum results in an error⁶ of 0.24 dex for $\log \epsilon(\text{Th}/\text{Eu})$, and therefore it was not possible to derive a meaningful age for CS 29497–004 using the Th/Eu chronometer. Furthermore, as we discussed in the introduction, it is unclear if Th/Eu is a useful chronometer at all.

It is likely that many more neutron-capture elements can be measured with higher resolution and S/N spectra. Such spectra have already been obtained with VLT/UVES. The low carbon abundance ($\log \epsilon(\text{C}) = 5.86$) and high level of enrichment

⁶ The error analysis procedure described in the Appendix of Paper II was employed.

with *r*-process elements also make CS 29497–004 a good candidate for an attempt to detect uranium.

We measure $[Fe/H] = -2.64 \pm 0.12$ for CS 29497–004, suggesting that this star is significantly more metal-rich than the three previously known *r*-II stars, CS 22892–052, CS 31082–001 and CS 22183–031 which all have $[Fe/H] \sim -3.0$. This would have important consequences for future searches for *r*-II stars, because it would mean that one should focus on the metallicity regime $[Fe/H] \lesssim -2.5$. However, for our analysis of CS 29497–004 we adopt a temperature scale which is slightly higher than that used in other studies (see Cohen et al. 2002, for a discussion). The homogenous analysis of CS 31082–001, CS 29497–004, and CS 22892–052 presented in Paper II in fact indicates that CS 29497–004 has a metallicity in between that of CS 31082–001 and CS 22892–052 (see Table 1 of Paper II).

In order to determine the boundaries of the metallicity range in which *r*-II stars can be found, we are endeavouring in the HERES effort to explore the region $-2.0 < [Fe/H] < -2.5$ with a statistically significant and homogeneously analysed sample of stars.

Acknowledgements. We are grateful to the ESO staff at Paranal and Garching for obtaining the VLT/UVES observations and reducing the data, respectively. Computations of tailored MARCS models by M. Mizuno-Wiedner, B. Edvardsson and B. Gustafsson are acknowledged. We are grateful to K. Eriksson and B. Edvardsson for technical help with the abundance analysis programs, and B. Gustafsson for many valuable comments. J. Cohen kindly derived an effective temperature for CS 29497–004 from broad-band photometry for us. We are indebted to A. Frebel for careful proofreading of an earlier version of the manuscript. N.C. acknowledges financial support through a Henri Chretien International Research Grant administered by the American Astronomical Society, from Deutsche Forschungsgemeinschaft under grants Re 353/44-1 and CH 214/3-1, and a Marie Curie Fellowship of the European Community program *Improving Human Research Potential and the Socio-Economic Knowledge* under contract number HPMF-CT-2002-01437. T.C.B. acknowledges partial funding for this work from grants AST 00-98508 and AST 00-98549 awarded by the US National Science Foundation and from award PHY 02-16783, Physics Frontiers Center/Joint Institute for Nuclear Astrophysics (JINA). P.B. acknowledges the support of the Swedish Research Council. A.J.K. acknowledges support from the Studienstiftung des deutschen Volkes and the Akademie Leopoldina under grant BMBF-LPD 9901/8-87. S.R. thanks the Brazilian Institutions FAPESP and CNPq for partial financial support. The work by G.J.W. was supported by DOE DE-FG03-88ER 13851, Caltech Division Contribution No. 9011(1116).

References

- Arlandini, C., Käppeler, F., Wisshak, K., et al. 1999, *ApJ*, 525, 886
 Auer, L., & Heasley, J. 1976, *ApJ*, 205, 165
 Barklem, P., Christlieb, N., Beers, T., et al. 2004, in preparation (Paper II)
 Beers, T. C. 1999, in *The Third Stromlo Symposium: The Galactic Halo*, ed. B. Gibson, T. Axelrod, & M. Putman, ASP Conf. Ser., 165, 202
 Beers, T. C., Preston, G. W., & Shectman, S. A. 1992, *AJ*, 103, 1987
 Beers, T. C., Rossi, S., Norris, J. E., Ryan, S. G., & Shefler, T. 1999, *AJ*, 117, 981
 Burris, D., Pilachowski, C., Armandroff, T., et al. 2000, *ApJ*, 544, 302
 Cayrel, R., Hill, V., Beers, T., et al. 2001, *Nature*, 409, 691
 Cayrel, R., Depagne, E., Spite, M., et al. 2004, *A&A*, 416, 1117
 Christlieb, N. 2003, *Rev. Mod. Astron.*, 16, 191
 [arXiv:astro-ph/0308016]
 Christlieb, N., Wisotzki, L., Reimers, D., et al. 2001, *A&A*, 366, 898
 Cohen, J., Christlieb, N., Beers, T., Gratton, R., & Carretta, E. 2002, *AJ*, 124, 470
 Cohen, J., Christlieb, N., Qian, Y., & Wasserburg, G. 2003, *ApJ*, 588, 1082
 Cowan, J., Sneden, C., Burles, S., et al. 2002, *ApJ*, 572, 861
 Cowan, J. J., McWilliam, A., Sneden, C., & Burris, D. L. 1997, *ApJ*, 480, 246
 Cowan, J. J., Pfeiffer, B., Kratz, K.-L., et al. 1999, *ApJ*, 521, 194
 Dekker, H., D’Odorico, S., Kaufer, A., Delabre, B., & Kotzlowski 2000, in *Optical and IR Telescope Instrumentation and Detectors*, ed. M. Iye, & A. F. Moorwood, 4008, 534
 Gehren, T. 1975a, *LTE-Sternatmosphärenmodelle (I)*, Tech. Rep., Universität Kiel
 Gehren, T. 1975b, *LTE-Sternatmosphärenmodelle (II)*, Tech. Rep., Universität Kiel
 Gustafsson, B., Edvardsson, B., Eriksson, K., et al. 2004, *A&A*, in preparation
 Hill, V., Barbuy, B., Spite, M., et al. 2000, *A&A*, 353, 557
 Hill, V., Plez, B., Cayrel, R., et al. 2002, *A&A*, 387, 560
 Honda, S., Aoki, W., Ando, H., et al. 2004a, *ApJS*, 152, 113
 Honda, S., Aoki, W., Kajino, T., et al. 2004b, *ApJ*, 607, 474
 Irwin, A. 1981, *ApJS*, 45, 621
 Johnson, J., & Bolte, M. 2001, *ApJ*, 554, 888
 Kamp, I., Korotin, S., Mashonkina, L., Przybilla, N., & Shimansky, V. 2004, in *Modelling of Stellar Atmospheres*, ed. N. Piskunov, W. Weiss, & D. Gray, IAU Symp., 210, 323
 Korn, A., Shi, J., & Gehren, T. 2003, *A&A*, 407, 691
 Kupka, F., Piskunov, N., Ryabchikova, T., Stempels, H., & Weiss, W. 1999, *A&AS*, 138, 119
 Kupka, F., Piskunov, N., Ryabchikova, T., Stempels, H., & Weiss, W. 2000, *Baltic Astronomy*, 9, 590
 Mashonkina, L., & Gehren, T. 2000, *A&A*, 364, 249
 Mashonkina, L., & Gehren, T. 2001, *A&A*, 376, 232
 Mashonkina, L., Gehren, T., & Bikmaev, I. 1999, *A&A*, 343, 519
 McWilliam, A., Preston, G., Sneden, C., & Searle, L. 1995, *AJ*, 109, 2757
 Morell, O., Kallander, D., & Butcher, H. 1992, *A&A*, 259, 543
 Nilsson, H., Zhang, Z., Lundberg, H., & Nordström, B. 2002, *A&A*, 382, 368
 Norris, J., Ryan, S., & Beers, T. 1999, *ApJS*, 123, 639
 Norris, J. E., Ryan, S. G., & Beers, T. C. 1997, *ApJ*, 489, L169
 Qian, Y.-Z., & Wasserburg, G. 2001a, *ApJ*, 552, L55
 Qian, Y.-Z., & Wasserburg, G. 2001b, *ApJ*, 559, 925
 Qian, Y.-Z., & Wasserburg, G. 2002, *ApJ*, 567, 515
 Ryan, S., & Norris, J. 1991, *AJ*, 101, 1865
 Schatz, H., Toenjes, R., Pfeiffer, B., et al. 2002, *ApJ*, 579, 626
 Schlegel, D., Finkbeiner, D., & Davis, M. 1998, *ApJ*, 500, 525
 Skrutskie, M., Schneider, S., Stiening, R., et al. 1997, in *The Impact of Large Scale Near-IR Sky Surveys*, ed. F. Garzón, N. Epchtein, A. Omont, W. Burton, & P. Persi (Dordrecht: Kluwer), 25
 Sneden, C., McWilliam, A., Preston, G. W., et al. 1996, *ApJ*, 467, 819
 Sneden, C., Cowan, J., Ivans, I., et al. 2000, *ApJ*, 533, L139
 Sneden, C., Cowan, J., Lawler, J., et al. 2003, *ApJ*, 591, 936
 Wanajo, S., Itoh, N., Ishimaru, Y., Nozawa, S., & Beers, T. 2002, *ApJ*, 577, 853
 Westin, J., Sneden, C., Gustafsson, B., & Cowan, J. 2000, *ApJ*, 530, 783
 Yi, S., Demarque, P., Kim, Y., et al. 2001, *ApJS*, 136, 417